HHS Public Access

Author manuscript

Angiogenesis. Author manuscript; available in PMC 2018 May 17.

Published in final edited form as:

Angiogenesis. 2015 April ; 18(2): 175–189. doi:10.1007/s10456-014-9455-0.

Tipping off endothelial tubes: nitric oxide drives tip cells

Mani Krishna Priya,
AU-KBC Research Centre, MIT Campus of Anna University, Chennai, India

Giriraj Sahu,
Department of Biotechnology, IIT Madras, Chennai, India

David R. Soto-Pantoja,
Laboratory of Pathology, Center for Cancer Research, National Cancer Institute, National Institutes of Health, Bethesda, MD, USA

Naga Goldy,
AU-KBC Research Centre, MIT Campus of Anna University, Chennai, India

Abaya Meenakshi Sundaresan,
AU-KBC Research Centre, MIT Campus of Anna University, Chennai, India

Vivek Jadhav,
AU-KBC Research Centre, MIT Campus of Anna University, Chennai, India

T. R. Barathkumar,
AU-KBC Research Centre, MIT Campus of Anna University, Chennai, India

Uttara Saran,
AU-KBC Research Centre, MIT Campus of Anna University, Chennai, India

B. M. Jaffar Ali,
Centre for Green Energy Technology, Pondicherry University, Pondicherry, India

David D. Roberts,
Laboratory of Pathology, Center for Cancer Research, National Cancer Institute, National Institutes of Health, Bethesda, MD, USA

Amal Kanti Bera, and
Department of Biotechnology, IIT Madras, Chennai, India

Suvro Chatterjee
AU-KBC Research Centre, MIT Campus of Anna University, Chennai, India. Department of Biotechnology, Anna University, Chennai, India

Abstract

Angiogenesis, the formation of new blood vessels from pre-existing vessels, is a complex process that warrants cell migration, proliferation, tip cell formation, ring formation, and finally tube

Correspondence to: Suvro Chatterjee.

Electronic supplementary material The online version of this article (doi:10.1007/s10456-014-9455-0) contains supplementary material, which is available to authorized users.

formation. Angiogenesis is initiated by a single leader endothelial cell called “tip cell,” followed by vessel elongation by “stalk cells.” Tip cells are characterized by their long filopodial extensions and expression of vascular endothelial growth factor receptor-2 and endocan. Although nitric oxide (NO) is an important modulator of angiogenesis, its role in angiogenic sprouting and specifically in tip cell formation is poorly understood. The present study tested the role of endothelial nitric oxide synthase (eNOS)/NO/cyclic GMP (cGMP) signaling in tip cell formation. In primary endothelial cell culture, about 40 % of the tip cells showed characteristic sub-cellular localization of eNOS toward the anterior progressive end of the tip cells, and eNOS became phosphorylated at serine 1177. Loss of eNOS suppressed tip cell formation. Live cell NO imaging demonstrated approximately 35 % more NO in tip cells compared with stalk cells. Tip cells showed increased level of cGMP relative to stalk cells. Further, the dissection of NO downstream signaling using pharmacological inhibitors and inducers indicates that NO uses the sGC/cGMP pathway in tip cells to lead angiogenesis. Taken together, the present study confirms that eNOS/NO/cGMP signaling defines the direction of tip cell migration and thereby initiates new blood vessel formation.

Keywords

Tip cell; Stalk cell; Nitric oxide; Endothelial nitric oxide synthase; Cyclic guanosine monophosphate

Introduction

Angiogenesis is defined as the formation of new blood vessels from pre-existing ones, which involves extracellular matrix degradation, migration, proliferation, differentiation, and tube formation [1]. Angiogenic sprouting is a guided process, where endothelial tip cells lead the vascular sprouting, and trailing stalk cells mediate lumen formation [2, 3]. Vascular endothelial growth factor (VEGF) guides angiogenic sprouting by inducing filopodia-like extensions in tip cells [2]. Selection of tip and stalk cells is regulated by Dll4/Notch signaling [4]. Earlier studies have shown higher expression of several angiogenic gene such as VEGFR2 [2], VEGFR3 [5], Dll4, and PDGF-B in the tip cells compared with that in stalk cells [3].

Several reports indicate that the nitric oxide synthase (NOS) pathway plays a significant role in angiogenesis [6, 7]. Nitric oxide (NO) donors, such as sodium nitroprusside, promote endothelial cell proliferation and migration in vivo and in vitro, while inhibitors of NOS suppress these responses [6]. Reports suggest that the growth-promoting effect of NO is linked to cGMP generation in cultured endothelium [8]. NO mediates the pro-angiogenic response of several key factors including VEGF, angiopoetin-2, and estrogen. These factors mediate their effects by phosphorylating endothelial NOS (eNOS) at Ser-1179, which provides a sustained flux of NO through overcoming its calmodulin dependence and is associated with pro-angiogenic responses [9]. In our earlier report, we have demonstrated that eNOS/NO/cGMP promotes ring formation [10], which is an early event of angiogenesis. However, the role of NO in tip cell sprouting is not understood yet. The present study reveals that polarization of eNOS and NO release directs the tip cell formation. Furthermore, ex

vivo eNOS knockout mouse experiments confirmed that functional eNOS is crucial for optimal tip cell sprouting. We also show that eNOS-derived NO mediates the tip cell sprouting via the sGC–cGMP pathway.

Materials and methods

Materials

Dulbecco's modified Eagle's medium (DMEM), fetal bovine serum (FBS), penicillin, and streptomycin were purchased from PAN-Biotech GmbH (Am Gewerbepark, Aidenbach). VEGF, (10 ng/mL), bradykinin (BK; 1 μM), diethylenetriamine NONOate (DEAN; 10 μM), 1*H*-[1,2,4]-oxidiazolo[4,3a]quinozalin-1-one (ODQ; 10 μM), guanosine-3′5-monophosphate 8-bromo-sodium salt (8-Br-cGMP; 50 μM), sildenafil citrate (SC; 1 μM), L-nitro-L-arginine-methyl ester (L-NAME; 1 mM), 2,3,9,10,11,12-hexahydro-10R-methoxy-2,9-dimethyl-1-oxo-9S,12R-epoxy-1*H*-diindolo[1,2,3-fg:3′, 2′,1′-kl]pyrrolo[3,4-i] [1, 6] benzodiazocine-10-carboxylic acid, methyl ester (KT5823; 1 μM), N_{ω}-nitro-D-arginine methyl ester hydrochloride (D-NAME; 1 mM), diaminorhodamine-4M-AM (DAR-4M-AM; 5 μM) were purchased from Sigma Chemical Co., St. Louis, MO, USA. Acetylcholine (Ach; 5 μM; Himedia), 2-phenyl-4,4,5,5-tetramethylimidazoline-1-oxyl 3-oxide (cPTIO; 10 μM; Calbiochem), myosin light chain kinase inhibitor (MLCKi; 30 μM; Santa Cruz, USA), phalloidin and DAPI were purchased from Invitrogen, USA. Caveolin-1 scaffolding domain peptide (CSP; 14 μM) was purchased from Merck Millipore, Germany. DETA NONOate (DETA) was purchased from Cayman Chemical, USA. All other chemicals used in this study were of the reagent grade and were obtained commercially.

Cell culture

The immortalized endothelial hybrid cell line EA.hy926 (kind gift from Dr. C.J.S. Edgell, University of North Carolina, Chapel Hill), the T24 bladder carcinoma cell line formerly designated ECV 304, which functionally mimics several endothelial functions [11], and T24/ECV 304 stably transfected with eNOS-GFP were kind gifts from Dr. Vijay Shah, Mayo Clinic, Rochester, USA. The cells were cultured in DMEM medium supplemented with 10 % FBS (v/v) and 1 % penicillin/streptomycin (w/v). The cells were maintained at 37 °C in a humidified CO_2 incubator.

Bovine endothelial cell isolation

Bovine aortic endothelial cells (BAECs), bovine lung microvascular endothelial cells (BMECs), and bovine pulmonary aortic endothelial cells (BPAECs) were isolated from bovine aortas, lungs, and pulmonary artery, respectively. Bovine aortas, lungs, and pulmonary arteries were collected from a government authorized slaughter house. BAECs, BMECs, and BPAECs were isolated according to protocols described elsewhere [12, 13]. Isolated cells were confirmed as endothelial cells by using antibody against endothelial marker eNOS. Primary endothelial cells were used till passage 6.

Tip cell formation in Matrigel

BAECs, BMECs, T24/ECV 304 eNOS-GFP, and EA.hy926 cells were used for tip cell formation study. BAEC was used for immunofluorescence experiments, and T24/ECV 304

eNOS-GFP was used for eNOS polarization and AFM experiments, whereas EA.hy926 was extensively used throughout the study. Endothelial cells of different confluences (10, 20, 40, 60, 80, and 100 %) were seeded on Matrigel-coated 12-well plate coverslips and allowed to solidify in 37 °C CO_2 incubator for 30 min. Endothelial cells were seeded on the top of the Matrigel, and tip cell formation was observed after 24 h of incubation. After 24 h, optimal numbers of tip cells were observed using 40 % confluence, and this cell density was selected to perform experiments for the entire study (Fig. 1a). The tip cells were identified as a leading cell with characteristic filopodial extensions and over-expression of tip cell marker endocan (Fig. 1c).

Tip cell formation assay was performed to analyze the tip cell forming capability under different treatment conditions. 40 % confluent EA.hy926 cells were seeded on the Matrigel-coated coverslips. NO pathway signaling was analyzed using various pharmacological inducers and inhibitors such as 8-bromo-cGMP (50 μM), sildenafil citrate (1 μM), ODQ (10 μM), KT (1 μM), MLCKi (30 μM), and the combination treatment of ODQ + DEAN, KT + DEAN, and MLCKi + DEAN. The cells were treated with the respective compounds after 4 h of cell seeding and continued until the end of the experiment. After 24 h, tip cell numbers were manually counted as a double-blind study.

NO imaging using DAR

EA.hy926—Forty percent of confluent EA.hy926 cells were seeded on Matrigel-coated 12-well plate coverslips. Cells were treated with DEAN (10 μM) or cPTIO after 4 h of cell seeding. After 24 h of treatment, the cells were incubated with NO-specific fluorescence probe DAR-4M-AM (5 μM) for 10 min. Monolayers were washed with 1× PBS, and cells were imaged using a fluorescence microscope with attached DP71 camera. The fluorescence intensity of the cells was calculated using Adobe Photoshop version 7.0.

Chick aortic ring sprouting

Chick aortic ring assay was performed as described elsewhere [14]. Briefly, chick aortic arches were cut from the heart under sterile conditions. 50 μL of Matrigel was placed on the coverslips and allowed to solidify for 30 min at 37 °C in a CO_2 incubator. Aortic arches were cut into small rings placed on the top of the Matrigel, and further 20 μL of Matrigel was again placed on the top of the aortic ring. After 4 h, NO donor, inhibitor, and scavenger such as DEAN, L-NAME, and cPTIO were added to the respective aortic explants and incubated for 36 h. The treatment was provided till the end of the experiment. After 36 h, the chick aortic rings were incubated with the NO-specific fluorescence indicator DAR-4M-AM for 20 min. The arches were gently washed using 1× PBS, and images were captured using Olympus microscope with attached DP71 camera. The fluorescence intensity of the DAR images was calculated using Adobe Photoshop version 7.0. Endothelial cell identity was imaged using endocan (Supplementary Figure 1).

NO imaging in chick chorioallantoic membrane

Briefly, fourth day fertilized eggs were broke open in a sterile petri dish. The vascular beds were incised out using a sterile scissor, and 1× PBS wash was provided. Treatments, which include control, DEAN, L-NAME, L-NAME + DEAN, and cPTIO, were provided in the

media and added to the respective vascular bed and incubated for 30 min. After 30 min of treatment, the vascular bed was incubated with NO-specific fluorescence probe DAR 4M-AM (5 μM) for further 30 min. 1× PBS wash was provided, and the sprouting edges on the vascular bed were chosen for imaging. The images were captured using Olympus microscope with attached DP71 camera. DAR-nitric oxide hot spots, which represent equivalent eNOS localization, were counted manually as a double-blinded study, and the graph is plotted.

Caveolin scaffolding peptide and NO release

EA.hy926 cells were seeded on Matrigel-coated 12-well plate coverslips. DEAN [10 μM], caveolin scaffolding peptide [CSP; 14 μM], L-NAME, and cPTIO drug treatment were provided in the media. Number of tip cells was counted manually as a double-blinded study.

Immunofluorescence

Immunofluorescence studies were carried out in BAECs. Endothelial tip cells were grown on Matrigel-coated 12-well coverslips. After 24 h, the cells were fixed in 2 % paraformaldehyde for 10 min and washed in 1× PBS. Then the cells were permeabilized using 0.1 % Triton-X and blocked using 5 % BSA for 1 h. After a 1× PBS wash, and the cells were incubated with the following primary antibodies: Rabbit polyclonal VEGFR2 (Abcam, USA), Human endocan (Lunginnov, France), rabbit polyclonal eNOS (Santa Cruz, USA), rabbit polyclonal anti-serine 1177 phosphorylated eNOS antibody (Abcam, USA), mouse monoclonal anti-caveolin (Abcam, USA), rabbit polyclonal nitrocysteine (Abcam, USA) all using 1:1,000 dilutions. The corresponding anti-mouse or anti-rabbit secondary antibodies tagged with FITC for VEGFR2, endocan, caveolin, nitrocysteine, and TRITC for eNOS, P-eNOS (1:2,000 dilutions) were added, and incubated for 2 h. The nuclei were stained using DAPI. The images were captured using an Olympus fluorescence microscope with an attached DP71 camera.

Phalloidin staining

EA.hy926 cells were seeded on Matrigel-coated 12-well plate coverslips. The cells were allowed to form tip cells under various treatments such as DEAN, L-NAME, L-NAME + DEAN, and cPTIO. After 24 h of tip cell formation, the cells were fixed and incubated with phalloidin for 30 min. Nuclear staining was done using DAPI. Images were captured using the Olympus 1X71 epifluorescence microscopy equipped with a DP71 camera.

eNOS siRNA transfection

EA.hy926 cells were transfected with eNOS siRNA (Sigma) using Lipofectamine 2000 (Invitrogen). Scrambled RNA was used as the control. eNOS siRNA and scrambled RNA-transfected cells were seeded on Matrigel and allowed to form tip cells. Numbers of tip cell were counted manually, and the bright field images were captured with an inverted microscope. eNOS siRNA transfection was confirmed using Western blot analysis probed for eNOS.

Western blot

Briefly, EA.hy926 cells were harvested and lysed in lysis buffer. Proteins were resolved in SDS-PAGE followed by transfer to nitrocellulose membrane [15]. Protein expression was analyzed using anti-eNOS antibody (NOS3, rabbit polyclonal, Santa Cruz Biotechnology Inc.).

Atomic force microscopy

T24/ECV 304, T24/ECV 304 eNOS-GFP cells, and BPAECs were chosen for topographic analysis. Once the endothelial cells attained tip cell conformation in Matrigel, the cells were fixed in 2 % paraformaldehyde for 10 min and washed in 1× PBS. Coverslips with fixed slides were then scanned with an atomic force microscopy using a nanoscope (Digital instruments) and the following parameters: scan size 100 μm, scan rate 3.052 Hz, height data scale 6 μm, engage X position 19783.4 μm, engage Y position 42,151.3 μm.

MATLAB image analysis

eNOS and NO fluorescence images were captured in fluorescence microcopy, and the images were processed in MATLAB for fluorescence intensity calculation. 50 images were processed for data analysis.

Chick aortic ring assay

The chick aortic ring assay was performed as mentioned above. Drug treatment (DEAN, L-NAME, cPTIO, and L-NAME + DEAN) was provided in the media, and the explants were imaged after 36 h of incubation period. Images were taken in 4× and 20× magnification using Olympus microscope attached with DP71 camera. Image analysis was performed using Angioquant software. Number of rings and tubes were manually counted as a double-blind study.

Bright field and live chick aortic sprout imaging

Aortic arches were dissected from 12-day-old chick embryos, and the rings were placed on the top of the Matrigel as described above. DEAN and cPTIO was added in the media. Tip cell sprout formation was recorded in the presence and absence of NO donor and scavenger (DEAN and cPTIO). After 16 h, once the aortic ring starts sprouting, the tip cell response to control, DEAN, and cPTIO was imaged at intervals of 5 min for 3 h. The captured images were then processed for filopodial length and angle measurements using ImageJ software.

Statistical analysis

All the experiments were performed in triplicate or more ($n \geq 3$) as specified. Data are represented as mean ± SEM. Data were analyzed using one-way ANOVA, Student's t test, and Tukey post hoc tests. Data with p value smaller or equal to 0.05 were considered statistically significant.

Results

Role of angiogenic factors in tip cell formation

To study tip cell formation, BAECs, BMECs, EA.hy926, and T24/ECV-304 eNOS-GFP cells were seeded on Matrigel at different confluences. After 24 h, the maximum number of tip cells was observed at 40 % confluence (Fig. 1a). Therefore, 40 % confluence of cells was chosen for the entire study. Using the Matrigel tip cell model, 40, 23, and 12 % increases in tip cell numbers were observed after treatment with VEGF (10 ng/mL), bradykinin (1 μM), and acetylcholine (5 μM), respectively, whereas combination treatment of VEGF, bradykinin, and acetylcholine with L-NAME decreased the tip cell number by 50, 48, and 45 %, respectively (Fig. 1b). For all the experiments, drug treatment was provided in the media 4 h after seeding and was continued until the end of the experiment. Tip cells were characterized using the tip cell marker VEGFR2 and endocan. Expression of VEGFR2 and endocan was found to be high in tip cells compared with that of stalk cells (Fig. 1c, d), and the same cells also exhibited actin rich filopodial extensions (Fig. 1e).

Role of nitric oxide in tip cell formation

To investigate the role of NO in tip cell formation, diaminorhodamine-4M-AM (DAR) imaging was performed both in EA.hy926 cells and in chick aortic rings. Production of NO in tip cells was significantly higher than that in stalk cells (Fig. 2a, b). Interestingly, NO production was found toward the anterior progressive end of the tip cell, which shows that NO defines tip cell migration direction (Fig. 2c, d). We tested whether exogenous supply or scavenging of NO could modulate tip cell formation. Cells were treated with the NO donor DEAN (10 μM), the NOS inhibitor L-NAME (1 mM), or the NO scavenger cPTIO (10 μM). D-NAME (1 mM), an inactive enantiomer of L-NAME, was used as a negative control. Control and D-NAME-treated cells showed similar number of tip cell number (Supplementary Figure 2a). Drugs were applied 4 h after cell seeding and continued till the end of the experiment. Application of DEAN and cPTIO resulted in significant rise and attenuation of the intracellular NO level, respectively (Fig. 3a–c). DEAN-treated cells showed increased numbers of tip cells and filopodial extensions (Supplementary Figure 2b). On the other hand, cPTIO treatment resulted in morphological changes in tip cells as well as significant reduction of their numbers. Application of DEAN increased the tip cell number by 26 % (Fig. 3b), whereas cPTIO reduced it by 24 % [number of experiment ($n \geq 3$, $^{**}p<0.001$ vs control)]. Similar to the effect observed in cell line, in chick aortic ring assay, DEAN increased tip cell numbers by 30 % and L-NAME inhibited it by 33 %. Nevertheless, DEAN reversed the inhibitory effect of L-NAME by 20 % (Fig. 3d–f). The results suggest that NO is crucial for tip cell formation and filopodial extensions.

NO promotes tip cell formation in ex vivo

To elucidate the role of NO under ex vivo condition, DAR imaging was performed in the growing vessels of the chick vascular bed. DAR-nitric oxide hot spots, which represent equivalent eNOS localization, were counted manually as a double-blinded study, and the graph is plotted (Fig. 4). Number of NO hot spots was found to be increased under DEAN treatment; on the other hand, the number was found to be decreased under cPTIO treatment (Fig. 4). We tested the effect of NO in chick aortic tip cell formation. Results have shown

that the number of rings [10] and vascular junctions was found to be increased under DEAN treatment, whereas the number was found to be reduced under cPTIO. DEAN treatment increased the length and size of the tubules, whereas L-NAME and cPTIO reduced both (Fig. 5a–c). To further explore the importance of NO in tip cell sprout initiation, chick aortic tip sprout formation was recorded for 3 h, capturing images at 5 min intervals. 10 μM of DEAN/cPTIO was supplemented in every 30 min. Consistent with other studies, new sprout initiation and increase in filopodial length were observed under DEAN treatment, whereas cPTIO showed the opposite effect (Fig. 5d–f). This indicates that NO helps initiation of sprout formation.

eNOS localization defines the initiation of a new tip

To determine the role of eNOS in tip cell formation, BAECs were cultured on Matrigel-coated coverslips, and tip cell formation was observed after 24 h. Immunofluorescence studies revealed a higher level of eNOS expression in tip cells than that in stalk cells. eNOS was preferentially distributed in tip cell and in apex of the tip cell, suggesting an important role of eNOS in tip cell formation (Fig. 6a–c). Among the tip cells, eNOS present in the apex of the tip cell sproutings was manually counted. Tip cells which contain eNOS hot spots at the apex of the tip cells were defined as eNOS +ve tips and which do not have eNOS hot spots at the apex of the tip cells were defined as eNOS −ve tips. The representative bar graph shows a significant increase in eNOS +ve tip cells (Fig. 6d). eNOS expression at the apex of tip cell was found to coincide with endocan expression (Fig. 1d). Further, new filopodial formation from eNOS regions of the tip cells strongly suggests that eNOS directs where the filopodial extension takes place (Fig. 6c). Immunofluorescence studies showed a defined peri-nuclear anterior progressive eNOS localization pattern in tip cells (Fig. 6a, e, f), whereas posterior retrograde eNOS localization pattern was observed in stalk cells. eNOS localization above the nucleus is defined as anterior or progressive, and below the nucleus is defined as posterior or retrograde. The anterior localization pattern of eNOS in tip cells shows that eNOS defines the tip cell sprouting direction. Altogether defined peri-nuclear eNOS localization and eNOS hot spots at the apex of tip cell further validate that eNOS plays a prominent role in tip cell migration (Fig. 6). MATLAB image analysis further showed that the intensity of eNOS staining is higher in tip cells than stalk cells (Fig. 6g, h). Surface topographic analysis by AFM showed more filopodial extensions in eNOS rich primary endothelial cell (BPAEC), whereas in the T24/ECV-304 eNOS-GFP cell line, the filopodial number was less and no filopodia was observed in eNOS-deficient T24/ECV 304 cells (Fig. 7a). The results further proved the role of eNOS in tip cell filopodial formation, which helps in tip cell migration.

Transfection of cells with eNOS siRNA resulted in a 40 % reduction in tip cell number compared with the scrambled siRNA control (Fig. 7b, c). Western blot analysis of eNOS siRNA-transfected cells showed a significant reduction in eNOS protein expression (Fig. 7d, e). Aortic rings from wild type and eNOS knockout mice were assayed for endothelial sprouting. Sprouting from wild type aortic rings occurred earlier and more profusely than sprouting from eNOS knockout rings. Endothelial identity was performed using endocan (Fig. 7f, g). Exogenous addition of NO donor, DETA, could rescue tip cell sprouting in eNOS knockout rings, whereas addition of the NO scavenger cPTIO was unable to alter the

tip sprouting in eNOS knockout mice. Further inhibition of eNOS in EA.hy926 cells using L-NAME and scavenging of NO using caveolin scaffolding domain peptide (CSP) showed a 15 % reduction in tip cell number (Fig. 7h, i). The results show that blocking eNOS and NO reduces tip cell numbers.

Up-regulation of cGMP level in tip cells

At very low concentrations (pM- to low nM), NO exerts its activity by activating the sGC/cGMP/PKG pathway, whereas at higher concentration, it may nitrosylate cysteine residues of target proteins. To dissect the pathway involved in NO-induced tip cell formation, we measured cGMP level using FlincG-GFP. As shown in Fig. 8a–c, levels of cGMP were significantly higher in tip cells compared with stalk cells. cGMP expression was found to be higher in budding tip cell (Fig. 8b). Several pharmacological agents were used to identify the key players involved in NO–sGC pathway. The cell permeable cGMP analog 8-bromo-cGMP increased the number of tip cells by 30 %, whereas the phosphodiesterase inhibitor SC increased the number by 50 %. In the same line, the sGC inhibitor ODQ, the PKG inhibitor KT, and the myosin light chain kinase inhibitor reduced the tip cell numbers by 40, 44, and 39 %, respectively. Moreover, DEAN treatment reversed the inhibitory effects of ODQ, MLCKi, and KT by 22, 24, and 20 %, respectively (Fig. 8d, e). Nitrosylation pattern in tip cells and stalk cells was analyzed using nitrocysteine-targeted antibody. Nitrocysteine expression was found to be similar under control and DEAN treatment (Supplementary Figure 3).

NO activates tip cell formation by phosphorylating eNOS

Intracellular calcium imaging was performed to study the role of eNOS/calcium signaling in tip cells. As shown in Fig. 9a, application of bradykinin elevated the intracellular calcium immediately. However, the extent of calcium rise in tip cells was not significantly different from stalk cells. Although studies show that eNOS expression can be activated by intracellular-free calcium and phosphorylation [16], many reports emphasize that phosphorylation is required for eNOS activation [17–19]. Further, we examined the phosphorylation status of e-NOS using an antibody specific for e-NOS phosphorylated at serine 1177. Phosphorylated eNOS (p-eNOS) was detected in tip cells as well as in stalk cells. Interestingly, p-eNOS expression was found to be elevated in tip cells compared with that of stalk cells (Fig. 9b). p-eNOS serine 1177 hotspots were observed at the apex of the tip cells (Fig. 9c), further associating the active form of eNOS with tip cell sprouting. The involvement of active eNOS in tip cell formation was further confirmed by localizing caveolin. Immunofluorescence study revealed higher level of caveolin expression in stalk cells compared with that in tip cells, and caveolin was not co-localized with eNOS in tip cells, which shows that the active form of eNOS is involved in tip cell formation (Fig. 9d).

To check whether NO exerts its activity by altering ion flux across the membrane, we measured the whole cell current using patch clamp. Current–voltage (*I–V*) relationship generated from stalk cells and tip cells did not show any significant difference. Current amplitudes as well as pattern of the *I–V* curves appeared same in both types of cells, indicating identical expression of functional channels on their membrane. Nevertheless, quenching of NO by cPTIO did not alter *I–V* curves neither in stalk cells nor in tip cells,

suggesting NO-mediated effects do not involve in ion channel modulation (Supplementary Figure 4).

Discussion

The role of NO in early events of angiogenesis such as migration and proliferation of endothelial cells has been studied extensively [20, 21]. The present study establishes the importance of eNOS-derived NO in tip cell sprouting. Previous reports demonstrated that VEGF up-regulates eNOS activity [22–24], while endothelium-derived NO appears to play an important role in each step of angiogenesis. In the present study, we have examined eNOS activation and its downstream signaling targets in endothelial tip cells versus stalk cells. Agonists activate eNOS through multiple mechanisms: phosphorylation/dephosphorylation of specific residues, interaction with different proteins, S-nitrosylation, and specific sub-cellular localization [25–27]. Although these agonists are individually unique in their downstream signaling, they promote ultimately eNOS activation. Accordingly, we recorded differential effects of the agonists on tip cell formation (Fig. 1b). However, being multi-targeted agonists, they could have activated other downstream targets as well as promoting the tip cell formation. To test the requirement for NO in agonist-mediated tip cell formation, L-NAME was used to block agonist-mediated eNOS activation and tip cell dynamics in endothelial cells. The results of these experiments validate that eNOS activation is very critical in promoting the tip cells under the agonist treatments (Fig. 1b).

To test the NO dependency of tip cell formation, we provided NO donor, DEAN with a half life of 3 min, and cPTIO, a NO-specific scavenger. DEAN increased and cPTIO decreased the tip cell sprouting (Fig. 3). It is evident that EC migration, proliferation, and differentiation require an optimal eNOS activity [20, 21]. Muroharo et al. reported that eNOS knockout mice fail to induce neovascularization, while the study by Ando et al. [28] showed that deficiency of eNOS caused a decrease in retinal neovascularization. We also observed that the number of sprouts was less in eNOS-null aortic rings, whereas a treatment with NO donors could restore sprouting of eNOS-null aortic rings (Fig. 7f). All these studies including our work strongly suggest that NO plays a crucial role in sprouting angiogenesis. Tsutsui et al. [29] reported that depletion of all three isoforms of NOS causes many cardiovascular disorders such as hypertension, atherosclerosis, and hyperlipidemia but does not abolish angiogenesis completely. Hence, sprouting can also occur in the absence of NO stimulation, but is facilitated to some extent by NO. These observations strongly suggest that eNOS is not the sole source of NO in the vascular bed that confers support to sprouting activities.

Intricate modulation of surface topography of endothelial cells by specific extensions such as filopodia and lamellopodia of the tip cells is a critical step for the formation of sprouts. The surface topography study by AFM validated the importance of eNOS in filopodial extensions (Fig. 7a). Expression and localization of eNOS and MT1-MMP are specific to endothelial lamellopodia and filopodia, respectively [24]. Bulotta et al. [30] demonstrated that eNOS becomes concentrated in the ruffles of non-confluent cells, and particularly at the leading edge of migrating cells. A plethora of studies has demonstrated that sub-cellular

localization and trafficking of eNOS are critical to eNOS activation [18, 31]. However, eNOS localization pattern and associated protein in endothelial cells in perspective of tip cell formation have not previously been studied. Results of immunofluorescence study in the present work demonstrate a unique eNOS expression pattern in the filopodia of the tip cells, where eNOS co-localizes with endocan, a sprouting-associated biomarker (Fig. 1d). Endocan, the endothelial cell-specific molecule-1, is mainly expressed by endothelial cells, and its expression was found to be high in endothelial filopodia [32, 33]. Altogether eNOS and DAR experiments convincingly demonstrate that the eNOS at the progressive edge is functionally “hot” and may articulate the direction and ultra-structural pattern of tip cell front (Figs. 3, 6). We speculate that endocan defines the eNOS localization and polarization in tip cells by de-localizing caveolin-1 that ultimately helps eNOS activation in the apex of the tip cells.

eNOS has been shown to be localized in a specific domain of plasma membrane called caveolae and to interact with caveolin-1 through caveolin-1 scaffolding domain, which inhibits eNOS activity [34–36]. Studies have shown that caveolin scaffolding domain (CSD) could block NO-mediated vascular permeability and that it could block NO release in vitro and tumor angiogenesis in vivo [36, 37]. When we used CSP, we observed that CSP could reduce the number of tip cells in the testing matrix (Fig. 7h, i). The work of Ju et al. [35] demonstrated that direct interaction of eNOS with caveolin-1 inhibits the synthase activity. Similarly, the results of immunofluorescence study confirmed that caveolin-1 does not co-localize with eNOS in the filopodial extensions of tip cells but co-localizes mostly in stalk cells. This kind of unique and spatial segregation of eNOS from caveolin-1 possibly drives the formation of tip cell extensions with activated eNOS and NO production.

Several studies have demonstrated that constitutive eNOS expression can be activated by intracellular-free calcium, eNOS–caveolin interaction, enzyme translocation, and phosphorylation [15]. This suggested that tip cells may handle calcium signaling differently, but we found no difference of basal calcium level between tip cells and stalk cells (Fig. 9a). Also, both cells showed agonist-induced calcium rise to the same extent, indicating that calcium signaling machinery in tip cells is not different from stalk cells. Additionally, ionic currents recorded from tip cells are indistinguishable from stalk cells. These results indicate that eNOS activation in tip cells is independent of calcium influx. Earlier, it has been shown that phosphorylation of eNOS stimulates NO production even in the presence of low calcium [17–19]. The results of immunofluorescence study show an increase in eNOS phosphorylation (at serine 1177) in tip cells compared with that in stalk cells (Fig. 9b), which fortifies the concept of calcium-independent spatial eNOS activation in the tip cells.

VEGF-stimulated endothelial cell tube formation in vitro requires eNOS activation that leads to NO release and is reported to be dependent on the subsequent generation of the second messenger cGMP [38, 39]. NO exerts its effect by binding to the heme in soluble guanylate cyclase (sGC) that activates cGMP synthesis. The cGMP level was determined by using a cGMP biosensor, delta-FlincG [40]. We observed very specific cGMP activities in tip cells that further prove that tip cell formation is highly associated with NO–sGC–cGMP signaling (Fig. 8). Nitrosylation expression was also found be similar under both control and DEAN treatments (Supplementary Figure 3), which further states that tip cell formation is primarily

through NO–sGC–cGMP pathway. It has been reported that systemic cGMP enhancement augmented angiogenesis in ischemic rat brains [41]. Sildenafil and its role in angiogenesis are well documented [42, 43]. To assess the importance of sGC–cGMP pathway in the formation of tip cells, we probed NO–sGC–cGMP downstream signaling further, and the results demonstrate that tip cell formation is highly associated with NO–sGC–cGMP signaling.

In summary, the present study indicates that spatial distribution of cav-1 in tip and stalk cells defines the activation of eNOS in sub-cellular domains of the endothelial cells; and thereby helps to select the tip cells from the endothelial "crowd." We postulate that a well-programed molecular segregation of Cav-1 and eNOS occurs in caveolae domains of tip cells and more specifically in the plasma membrane of tips of the tip cells in a transient manner. A simultaneous surge in the level of cGMP in the micro-pockets of tip cells, and segregation of eNOS from Cav-1 transforms the micro-milieu into sGC–cGMP-dependent NO signaling pockets, which ultimately guide filopodial extensions by modulating actin polymerization (Supplementary Figure 5) to assist sprouting.

Supplementary Material

Refer to Web version on PubMed Central for supplementary material.

Acknowledgments

This project was partially supported by Grants from Indo-US Science and Technology Forum IUSSTF—R&D Center for "Cardiovascular Biology" (IUSSTF/JC/Cardiovascular Biology/62-2009/2010-2011), Intramural Research Program of the NIH/NCI (D.D.R.) and University Grant Commission-Faculty Recharge Program (UGC-FRP), Government of India to SC.

References

1. Pyriochou A, Zhou Z, Koika V, Petrou C, Cordopatis P, Sessa WC, Papapetropoulos A. The phosphodiesterase 5 inhibitor sildenafil stimulates angiogenesis through a protein kinase G/MAPK pathway. J Cell Physiol. 2007; 211:197–204. [PubMed: 17226792]
2. Gerhardt H, Golding M, Fruttiger M, Ruhrberg C, Lundkvist A, Abramsson A, Jeltsch M, Mitchell C, Alitalo K, Shima D, Betsholtz C. VEGF guides angiogenic sprouting utilizing endothelial tip cell filopodia. J Cell Biol. 2003; 161:1163–1177. [PubMed: 12810700]
3. Strasser GA, Kaminker JS, Tessier-Lavigne M. Microarray analysis of retinal endothelial tip cells identifies CXCR4 as a mediator of tip cell morphology and branching. Blood. 2010; 115:5102–5110. [PubMed: 20154215]
4. Suchting S, Freitas C, le Noble F, Benedito R, Bréant C, Duarte A, Eichmann A. The notch ligand delta-like 4 negatively regulates endothelial tip cell formation and vessel branching. Proc Natl Acad Sci USA. 2007; 104:3225–3230. [PubMed: 17296941]
5. Tammela T, Zarkada G, Wallgard E, Murtomäki A, Suchting S, Wirzenius M, Waltari M, Hellström M, Schomber T, Peltonen R, Freitas C, et al. Blocking VEGFR-3 suppresses angiogenic sprouting and vascular network formation. Nature. 2008; 454:656–660. [PubMed: 18594512]
6. Ziche M, Morbidelli L, Choudhuri R, Zhang HT, Donnini S, Granger HJ, Bicknell R. Nitric oxide synthase lies downstream from vascular endothelial growth factor-induced but not basic fibroblast growth factor-induced angiogenesis. J Clin Invest. 1997; 99:2625–2634. [PubMed: 9169492]
7. Fukumura D, Gohongi T, Kadambi A, Izumi Y, Ang J, Yun CO, Buerk DG, Huang PL, Jain RK. Predominant role of endothelial nitric oxide synthase in vascular endothelial growth factor-induced

angiogenesis and vascular permeability. Proc Natl Acad Sci USA. 2001; 98:2604–2609. [PubMed: 11226286]

8. Ziche M, Morbidelli L. Nitric oxide and angiogenesis. J Neurooncol. 2000; 50:139–148. [PubMed: 11245273]
9. Ridnour LA, Isenberg JS, Espey MG, Thomas DD, Roberts DD, Wink DA. Nitric oxide regulates angiogenesis through a functional switch involving thrombospondin-1. Proc Natl Acad Sci USA. 2005; 102:13147–13152. [PubMed: 16141331]
10. Sinha S, Sridhara SR, Srinivasan S, Muley A, Majumder S, Kuppusamy M, Gupta R, Chatterjee S. NO (nitric oxide): the ring master. Eur J Cell Biol. 2011; 90:58–71. [PubMed: 20800929]
11. Jones RA, Wang Z, Dookie S, Griffin M. The role of TG2 in ECV304-related vasculogenic mimicry. Amino Acids. 2013; 44:89–101. [PubMed: 22231926]
12. Ryan US. Isolation and culture of pulmonary endothelial cells. Environ Health Perspect. 1984; 56:103–114. [PubMed: 6090112]
13. Chung-Welch N, Shepro D, Dunham B, Hechtman HB. Prostacyclin and prostaglandin E2 secretions by bovine pulmonary microvessel endothelial cells are altered by changes in culture conditions. J Cell Physiol. 1988; 135:224–234. [PubMed: 2836441]
14. Siamwala JH, Veeriah V, Priya MK, Rajendran S, Saran U, Sinha S, Nagarajan S, Pradeep T, Chatterjee S. Nitric oxide rescues thalidomide mediated teratogenicity. Sci Rep. 2012; 2:679. [PubMed: 22997553]
15. Mukhopadhyay S, Shah M, Patel K, Sehgal PB. Mono-crotaline pyrrole induced megalocytosis of lung and breast epithelial cells: disruption of plasma membrane and Golgi dynamics and an enhanced unfolded protein response. Toxicol Appl Pharmacol. 2006; 211:209–220. [PubMed: 16000202]
16. Fleming I, Busse R. Signal transduction of eNOS activation. Cardiovasc Res. 1999; 43:532–541. [PubMed: 10690325]
17. Sessa WC, Garcia-Cardena G, Liu J, Keh A, Pollock JS, Bradley J, Thiru S, Braverman IM, Desai KM. The Golgi association of endothelial nitric oxide synthase is necessary for the efficient synthesis of nitric oxide. J Biol Chem. 1995; 270:17641–17644. [PubMed: 7543089]
18. Zhang Q, Church JE, Jagnandan D, Catravas JD, Sessa WC, Fulton D. Functional relevance of Golgi- and plasma membrane-localized endothelial NOS synthase in reconstituted endothelial cells. Arterioscler Thromb Vasc Biol. 2006; 26:1015–1021. [PubMed: 16514082]
19. McCabe TJ, Fulton D, Roman LJ, Sessa WC. Enhanced electron flux and reduced calmodulin dissociation may explain “calcium-independent” eNOS activation by phosphorylation. J Biol Chem. 2000; 275:6123–6128. [PubMed: 10692402]
20. Murohara T, Witzenbichler B, Spyridopoulos I, Asahara T, Ding B, Sullivan A, Losordo DW, Isner JM. Role of endothelial nitric oxide synthase in endothelial cell migration. Arterioscler Thromb Vasc Biol. 1999; 19:1156–1161. [PubMed: 10323764]
21. Guo J-P, Murohara T, Panday MM, Lefer AM. Nitric oxide promotes endothelial cell proliferation: role in inhibiting restenosis. Circulation. 1996; 92:I–750. Abstract.
22. van der Zee R, Murohara T, Luo Z, et al. Vascular endothelial growth factor/vascular permeability factor augments nitric oxide release from quiescent rabbit and human vascular endothelium. Circulation. 1997; 95:1030–1037. [PubMed: 9054767]
23. Hood JD, Meininger CJ, Ziche M, Granger HJ. VEGF upregulates ecNOS message, protein, and NO production in human endothelial cells. Am J Physiol. 1998; 274:H1054–H1058. [PubMed: 9530221]
24. Genís L, Gonzalo P, Tutor AS, Gálvez BG, Martínez-Ruiz A, Zaragoza C, Lamas S, Tryggvason K, Apte SS, Arroyo AG. Functional interplay between endothelial nitric oxide synthase and membrane type 1–matrix metalloproteinase in migrating endothelial cells. Blood. 2007; 110:2916–2923. [PubMed: 17606763]
25. Fulton D, Gratton JP, McCabe TJ, Fontana J, Fujio Y, Walsh K, Franke TF, Papapetropoulos A, Sessa WC. Regulation of endothelium-derived nitric oxide production by the protein kinase Akt. Nature. 1999; 399:597–601. [PubMed: 10376602]

26. Scotland RS, Morales-Ruiz M, Chen Y, Yu J, Rudic RD, Fulton D, Gratton JP, Sessa WC. Functional reconstitution of endothelial nitric oxide synthase reveals the importance of serine 1179 in endothelium-dependent vasomotion. Circ Res. 2002; 90:904–910. [PubMed: 11988492]
27. Erwin PA, Lin AJ, Golan DE, Michel T. Receptor-regulated dynamic s-nitrosylation of endothelial nitric-oxide synthase in vascular endothelial cells. J Biol Chem. 2005; 280:19888–19894. [PubMed: 15774480]
28. Ando A, Yang A, Mori K, Yamada H, Yamada E, Takahashi K, Saikia J, Kim M, Melia M, Fishman M, Huang P, Campochiaro PA. Nitric oxide is proangiogenic in the retina and choroid. J Cell Physiol. 2002; 191:116–124. [PubMed: 11920687]
29. Tsutsui M, Shimokawa H, Morishita T, Nakashima Y, Yanagihara N. Development of genetically engineered mice lacking all three nitric oxide synthases. J Pharmacol Sci. 2006; 102:147–154. [PubMed: 17031076]
30. Bulotta S, Cerullo A, Barsacchi R, De Palma C, Rotiroti D, Clementi E, Borgese N. Endothelial nitric oxide synthase is segregated from caveolin-1 and localizes to the leading edge of migrating cells. Exp Cell Res. 2006; 312:877–889. [PubMed: 16427620]
31. Chatterjee S, Cao S, Peterson TE, Simari RD, Shah V. Inhibition of GTP-dependent vesicle trafficking impairs internalization of plasmalemmal eNOS and cellular nitric oxide production. J Cell Sci. 2003; 116(Pt 17):3645–3655. [PubMed: 12876216]
32. Lassalle P, Molet S, Janin A, Heyden JV, Tavernier J, Fiers W, Devos R, Tonnel AB. ESM-1 is a novel human endothelial cell-specific molecule expressed in lung and regulated by cytokines. J Biol Chem. 1996; 271:20458–20464. [PubMed: 8702785]
33. Roudnicky F, Poyet C, Wild P, Krampitz S, Negrini F, Huggenberger R, Rogler A, Stöhr R, Hartmann A, Provenzano M, Otto VI, Detmar M. Endocan is upregulated on tumor vessels in invasive bladder cancer where it mediates VEGF-A-induced angiogenesis. Cancer Res. 2013; 73:1097–1106. [PubMed: 23243026]
34. Feron O, Belhassen L, Kobzik L, Smith TW, Kelly RA, Michel T. Endothelial nitric oxide synthase targeting to caveolae: specific interactions with caveolin isoforms in cardiac myocytes and endothelial cells. J Biol Chem. 1996; 271:22810–22814. [PubMed: 8798458]
35. Ju H, Zou R, Venema VJ, Venema RC. Direct interaction of endothelial nitric-oxide synthase and caveolin-1 inhibits synthase activity. J Biol Chem. 1997; 72:18522–18525.
36. Brouet A, Sonveaux P, Dessy C, Moniotte S, Balligand JL, Feron O. Hsp90 and caveolin are key targets for the proangiogenic nitric oxide—mediated effects of statins. Circ Res. 2001; 89:866–873. [PubMed: 11701613]
37. Bernatchez PN, Bauer PM, Yu J, Prendergast JS, He P, Sessa WC. Dissecting the molecular control of endothelial NO synthase by caveolin-1 using cell-permeable peptides. Proc Natl Acad Sci USA. 2005; 102:761–766. [PubMed: 15637154]
38. Papapetropoulos A, Garcia-Cardena G, Madri JA, Sessa WC. Nitric oxide production contributes to the angiogenic properties of vascular endothelial growth factor in human endothelial cells. J Clin Invest. 1997; 100:3131–3139. [PubMed: 9399960]
39. Bussolati B, Dunk C, Grohman M, Kontos CD, Mason J, Ahmed A. Vascular endothelial growth factor receptor-1 modulates vascular endothelial growth factor-mediated angiogenesis via nitric oxide. Am J Pathol. 2001; 159:993–1008. [PubMed: 11549592]
40. Nausch LW, Ledoux J, Bonev AD, Nelson MT, Dostmann WR. Differential patterning of cGMP in vascular smooth muscle cells revealed by single GFP-linked biosensors. Proc Natl Acad Sci USA. 2008; 105:365–370. [PubMed: 18165313]
41. Senthilkumar A, Smith RD, Khitha J, Arora N, Veerareddy S, et al. Sildenafil promotes ischemia-induced angiogenesis through a PKG-dependent pathway. Arterioscler Thromb Vasc Biol. 2007; 27:1947–1954. [PubMed: 17585066]
42. Aicher A, Heeschen C, Feil S, Hofmann F, Mendelsohn ME, Feil R, Dimmeler S. cGMP-dependent protein kinase I is crucial for angiogenesis and postnatal vasculogenesis. PLoS One. 2009; 4:e4879. [PubMed: 19287493]
43. Zhang R, Wang L, Zhang L, Chen J, Zhu Z, Zhang Z, Chopp M. Nitric oxide enhances angiogenesis via the synthesis of vascular endothelial growth factor and cGMP after stroke in the rat. Circ Res. 2003; 92:308–313. [PubMed: 12595343]

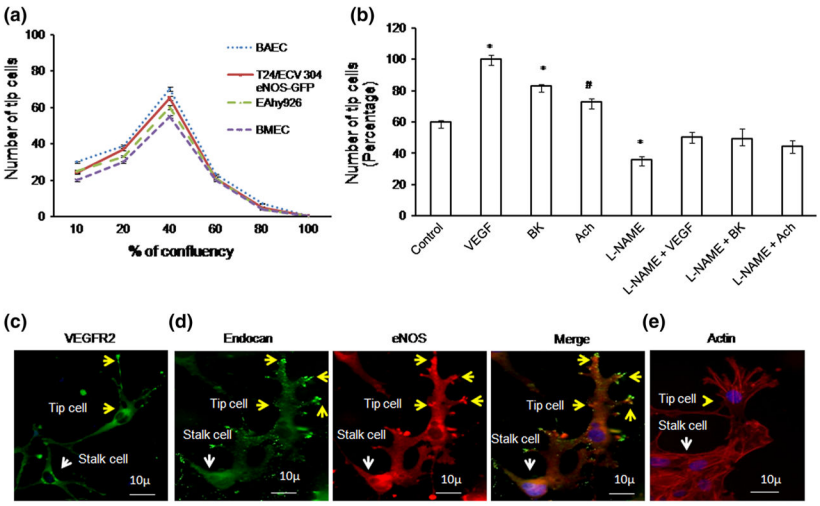

Fig. 1.

Tip cell characterization: **a** Endothelial cells (BAEC, BMEC, EA.hy926, and T24/ECV 304 eNOS-GFP) were seeded on the Matrigel-coated coverslips. Among various cell confluences, 40 % confluence allows effective tip cell sprouting ($n = 3$). Almost, BAEC, EA.hy926, and T24/ECV 304 eNOS-GFP showed similar number of tip cells. **b** Tip cell number was counted under various pro-angiogenic factors; VEGF, BK, and Ach above control and the combination of L-NAME + VEGF, L-NAME + BK, L-NAME + Ach. Significant increase in tip cell number was observed ($n = 3$; $^{*}p<0.001$ vs control, $^{\#}p = 0.027$ vs control). **c**, **d** Fluorescence imaging of tip cells in BAECs. Tip cells were characterized using known tip cell marker VEGFR2 and endocan. Immunofluorescence was carried out in BAEC. VEGFR2 was found to be high in tip cells than stalk cells. Endocan was tagged with FITC, and eNOS was tagged with TRITC. Endocan hot spots, which match with eNOS hot spots, were found to be more in tip cells (*yellow arrow mark*) than stalk cells (*white arrow mark*). **e** Representative actin rich filopodia in tip cells (*yellow arrow mark*) and stalk cells (*white arrow mark*); actin staining is shown in *red,* and DAPI staining is shown in *blue*. (Color figure online)

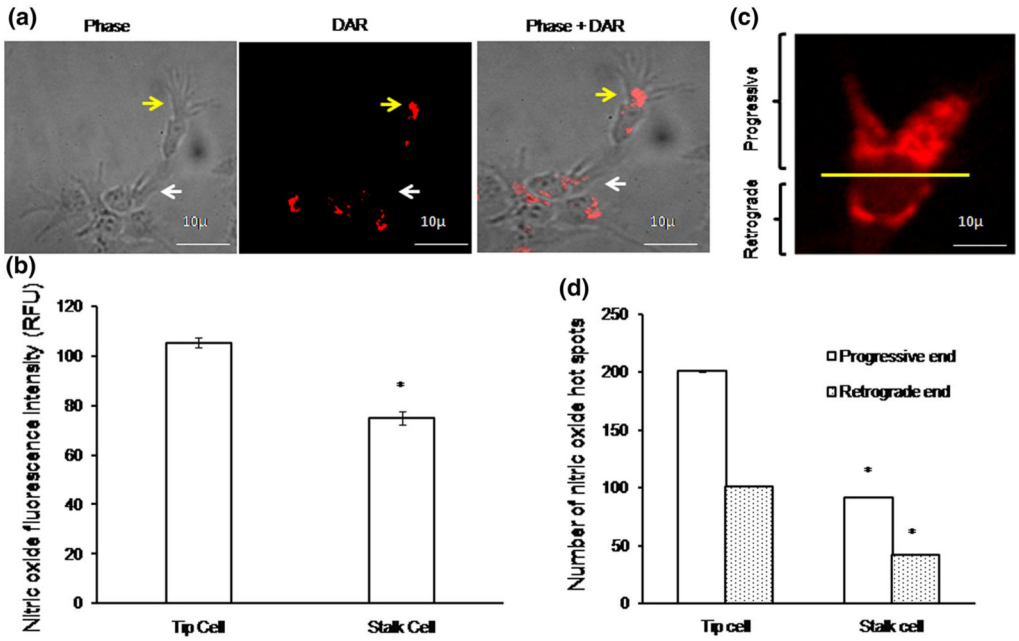

Fig. 2.

NO imaging using DAR: **a** EA.hy926 cells were incubated with NO-specific fluorescence probe DAR for 10 min, ×1 PBS wash was provided, and the images were captured using fluorescence microscope. Phase, DAR, and phase + DAR probed images of tip cell (*yellow arrow mark*) and stalk cell (*white arrow mark*). **b** Fluorescence intensity measurement, against NO, in tip cell and stalk cell was calculated using Adobe Photoshop version 7.0. Significant increase in NO fluorescence intensity was observed in tip cells than stalk cells ($n \geq 3$, $^*p<0.001$ vs tip cell). **c** Representative image shows the progressive (*upper part*) and retrograde end (*lower part*) within the tip cell. **d** Numbers of nitric oxide hot spots were counted in both tip cell and stalk cell progressive and retrograde ends, and the graph was plotted ($n>3$, $^*p = 0.001$). (Color figure online)

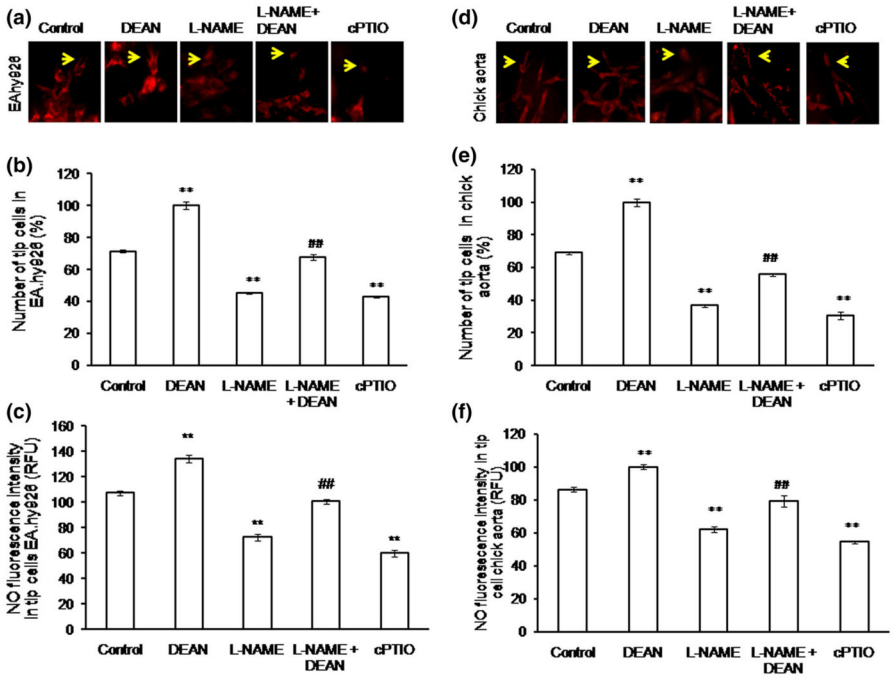

Fig. 3.

NO promotes tip cell formation in EA.hy926 and in chick aorta: **a** representative images of control, DEAN, L-NAME, L-NAME + DEAN, and cPTIO treatment in EA.hy926. After treatment, EA.hy926 cells were incubated with DAR, and the images were captured using fluorescence microscope. **b** EA.hy926 cells were subjected to form tip cells, and the number of tip cells was counted under DEAN (NO donor), NO scavenger and inhibitor (cPTIO and L-NAME) and the combination treatment of L-NAME + DEAN. A significant increase in tip cell number was observed under DEAN treatment, whereas L-NAME and cPTIO reduced the tip cell number ($n \geq 3$, $^{**}p<0.001$ vs control, $^{\#\#}p<0.05$ vs L-NAME). **c** NO in endothelial tip cells. EA.hy926 cells were treated with NO fluorescence probe DAR for 10 min, and the fluorescence images were taken. Fluorescence intensity was calculated using Adobe Photoshop version 7.0, and the graph was plotted ($n \geq 3$, $^{**}p<0.001$ vs control, $^{\#\#}p<0.05$ vs L-NAME). **d** Representative images of control, DEAN, L-NAME, L-NAME + DEAN, and cPTIO treatment in chick aorta. **e** DEAN treatment increased the tip cell sprouting in chick aortic rings. The tip cell number was significantly decreased in the presence of L-NAME and cPTIO ($n \geq 3$, $^{**}p<0.001$ vs control, $^{\#\#}p<0.05$ vs L-NAME). **f** Chick aortic rings were treated with DAR and incubated for 20 min, and the fluorescence intensity measurement was calculated using Adobe Photoshop 7.0. ($n \geq 3$, $^{**}p<0.001$ vs control, $^{\#\#}p<0.05$ vs L-NAME). (Color figure online)

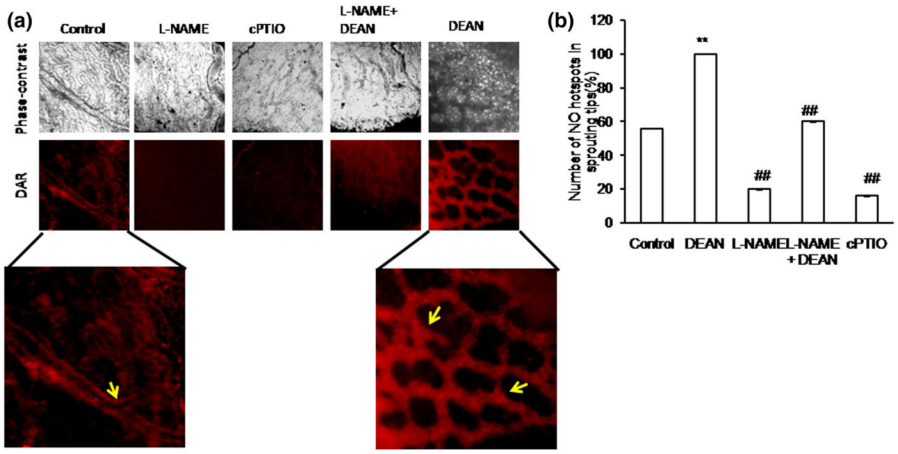

Fig. 4.

Ex vivo imaging of NO in chick vascular bed: **a** Fourth day eggs were broke open in a petri dish. The vascular beds were incised out using a sterile scissor, and ×1 PBS wash was provided. Treatments, which include control, DEAN, L-NAME, L-NAME + DEAN, and cPTIO, were provided in the media and incubated for 30 min. After 30 min of treatment, the vascular bed was then incubated with NO-specific fluorescence probe DAR4M-AM(5 μM)for 30 min.×1 PBS wash was provided, and the sprouting edges on the vascular bed were chosen for imaging. The images were captured using Olympus microscope attached with DP71 camera. The representative phase contrast and DAR images are provided. Control and DEAN images were magnified to highlight NO hot spots in the sprouting tips. **b** DAR-nitric oxide hot spots, which represent equivalent eNOS localization, were counted manually as a double-blinded study, and the graph is plotted. Nitric oxide hot spots were found to be significantly increased under DEAN treatment (** $p<0.001$ vs control), whereas NO hot spots were decreased when observed under L-NAME and cPTIO ($^{\#\#}p<0.05$ vs control). Combination treatment of DEAN could recover back the L-NAME-mediated inhibitory action ($^{\#\#}p<0.05$ vs L-NAME). (Color figure online)

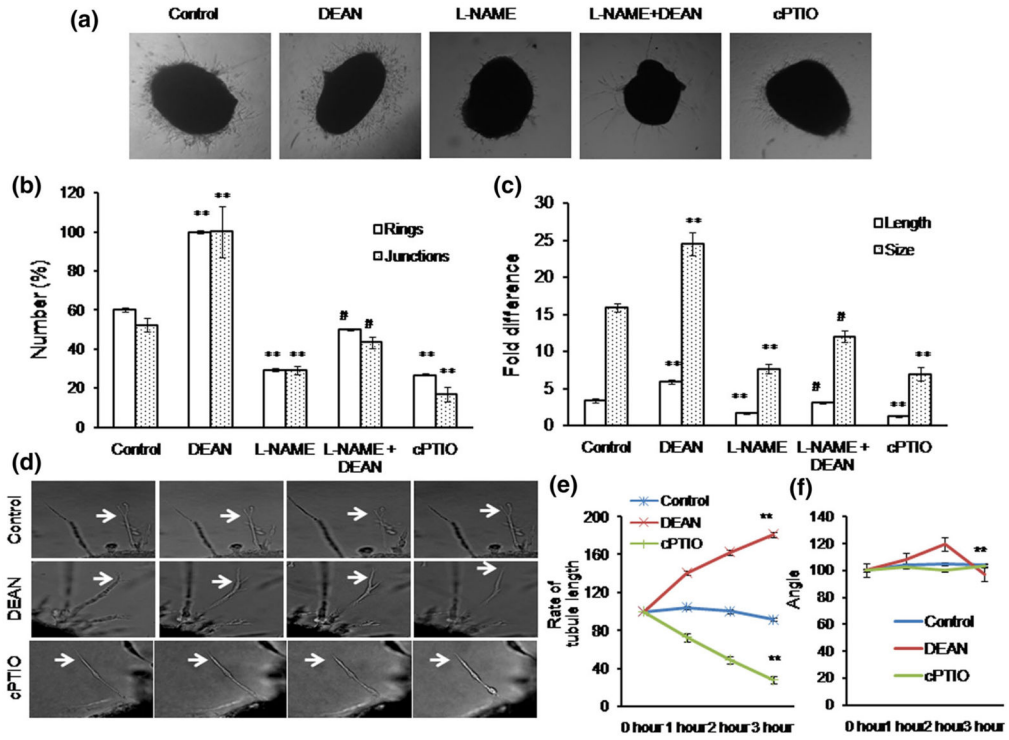

Fig. 5.

Chick aortic ring sprouting analysis: **a** 12-day-old chick embryo was killed, and aortas were cut into small pieces. The aortas were placed between the Matrigel, and drug treatment (DEAN, L-NAME, L-NAME + DEAN and cPTIO) was provided in the media. Angiogenic parameters such as number of rings [10], length and size of the tubule, and number of junctions were quantified and plotted ($n \geq 3$). **b** Significant increase in ring and junction number was quantified under DEAN treatment compared with control, whereas L-NAME and cPTIO decreased the number of rings and junction compared with control ($n \geq 3$, $^{**}p<0.001$ vs control and $^{\#}p<0.05$ vs L-NAME). **c** DEAN treatment increased the tip cell length and size, whereas L-NAME and cPTIO treatment decreased the tip cell length and size. Combination treatment of DEAN could recover back the L-NAME-mediated inhibitory effect. Values are represented as mean for each group ±SEM ($n>3$, $^{**}p<0.001$ vs control and $^{\#}p<0.05$ vs L-NAME). **d** The chick aortic ring experiment was performed as described in "Materials and methods" section. During the tip sprout initiation, the chick aortas were tracked for 3 h at an interval of 5 min, for DEAN and cPTIO, the treatment was provided every 30 min, and the images were captured. The tubule length and the angle were calculated using ImageJ software. **e**, **f** Compared to control, the tubule length and angle were increased under DEAN treatment, whereas the tubule length and angle were decreased under cPTIO ($n>3$, $^{**}p<0.001$ vs 0 h DEAN, cPTIO)

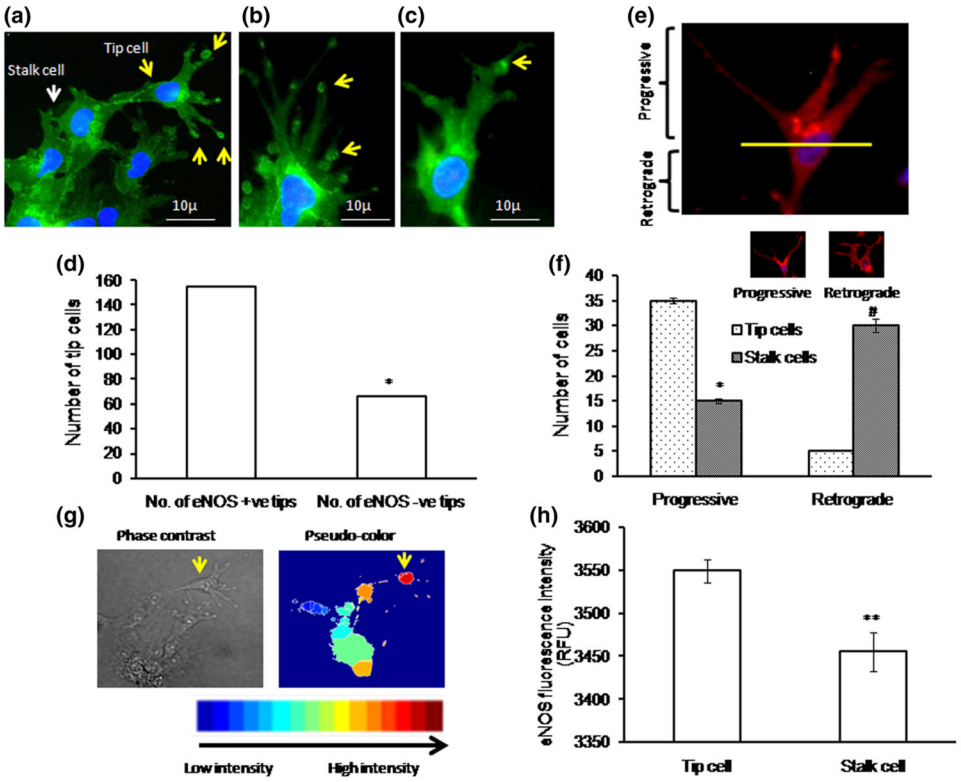

Fig. 6.

eNOS localization in tip cell: **a**–**c** eNOS immunofluorescence imaging shows that eNOS expression is high in tip cells and at the apex of the tip cells. eNOS hot spots were found to be more at the tip of the tip cells (*yellow arrow*) than the stalk cells (*white arrow*). Nuclear staining was done using DAPI (*blue color*). **d** Representative graph shows that within the tip cell, eNOS is highly enriched in the tip of the tip cell ($n \geq 3$, $^{*}p<0.05$ vs number of eNOS +ve tips). Tip cells which contain eNOS hot spots at the apex of the tip cells were defined as eNOS +ve tips and which do not have eNOS hot spots at the apex of the tip cells were defined as eNOS −ve tips. Based on the eNOS hot spots at the apex of the tip cells, eNOS +ve tip cells and eNOS −ve tip cells were manually counted as a double-blinded study. Almost 200 cells were chosen, and eNOS +ve and −ve tips were counted and plotted. **e** Fluorescence microscopic results showed the peri-nuclear progressive eNOS (Golgi) localization pattern in tip cells and retrograde eNOS (Golgi) localization pattern in stalk cells. eNOS localization above the nucleus is defined as progressive, and below the nucleus is defined as retrograde. **f** Representative graph shows significant increase in tip cell number toward progressive end ($n \geq 3$, $^{*}p<0.001$ vs tip cells progressive and $^{\#}p<0.001$ vs tip cell retrograde). **g** Immunofluorescence (eNOS) images were captured, and 50 images were processed in MATLAB software for image analysis. Pseudo-color was assigned to the bright field eNOS image to analyze the eNOS pattern in tip cells and stalk cells. **h** Graphical results showed high eNOS intensity in tip cells compared with that in neighboring stalk cells ($n \geq 3$, $^{**}p<0.001$ vs tip cells). (Color figure online)

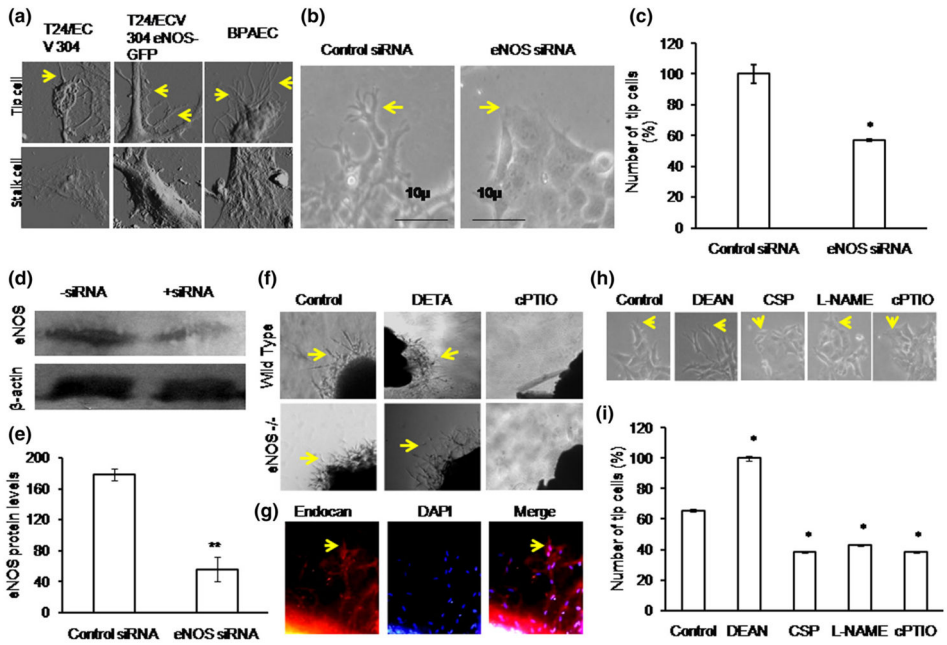

Fig. 7.

eNOS promotes tip cell formation: **a** Tip cells were fixed using 2 % paraformaldehyde and scanned using atomic force microscopy. AFM image results showed more filopodial extensions in BPAEC, less filopodial extensions in T24/ECV 304 eNOS-GFP, whereas no filopodia in eNOS-null T24/ECV 304. *Yellow color arrow mark* indicates the filopodial extensions. **b**, **c** At 36 h of transfection, the number of tip cells formed under both control siRNA and eNOS siRNA transfections were counted and plotted. Tip cell (indicated in *yellow color arrow mark*) number was significantly decreased under eNOS siRNA-transfected EA.hy926 cells than non-transfected EA.hy926 cells ($n = 3$, $^{*}p = 0.01$ vs control). **d** Representative Western blot results showed the transient knockdown of eNOS under eNOS siRNA treatment. **e** Control siRNA and eNOS siRNA protein expression levels were measured in three different sets of experiment ($^{**}p<0.001$ vs control siRNA). **f** Wild type and eNOS $KO^{-/-}$ mice aortas were cut into small pieces and placed between the Matrigel. After 48 h drug treatment, the images were captured in ×4 magnification using inverted microscope. *Yellow color arrow mark* indicates the tip cell sprouting. **g** Endothelial identity was imaged using endocan (*red*), nucleus stain was done using DAPI (*blue*), and their merged image is shown. *Yellow color arrow mark* indicates the tip cell sprouting. **h**, **i** EA.hy926 cells were allowed to form tip cells under DEAN, CSP, L-NAME, and cPTIO. Significant increase in tip cell number was observed under DEAN treatment, and similarly significant decrease in tip cell number was observed under CSP drug treatment. L-NAME and cPTIO reduced the tip cell formation ($n = 3$, $^{*}p<0.05$ vs control). (Color figure online)

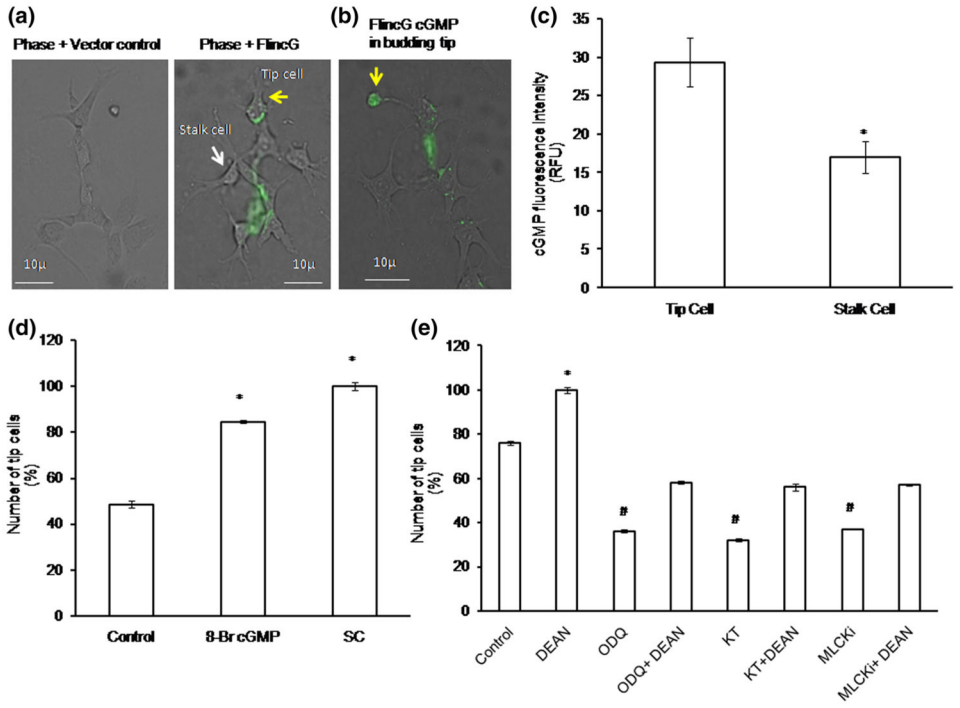

Fig. 8.

cGMP live imaging using FlincG and NO downstream pathway dissection: **a** EA.hy926 cells were electroporated with FlincG-GFP plasmid and allowed to form tip cells on the Matrigel-coated coverslips. After 36 h of transfection, the cells were treated with 10 μM of DEAN and live images were taken using fluorescence microscope. Representative images of phase + vector control and phase + FlincG transfected cells. *Yellow arrow mark* denotes tip cells, and *white arrow mark* denotes stalk cells. **b** Representative image shows that cGMP level was found to be high in the budding tip cell (*yellow arrow*). **c** cGMP fluorescence intensity calculations were analyzed using Adobe Photoshop 7.0. Tip cells showed high fluorescence intensity than stalk cells. The images are representative of ten different culture plates ($n>3$; $^{*}p = 0.002$ vs tip cells). **d** Compared to control, significant increase in tip cell number was observed under 8-Br-cGMP and SC ($n = 3$, $^{*}p<0.05$ vs control). **e** After 4 h of cell seeding, EA.hy926 cells were treated with NO downstream pharmacological inhibitors such as KT, ODQ, and MLCKi, and the number of tip cells was counted manually. Statistically significant decrease in tip cell number was observed under KT, ODQ, and MLCKi, whereas combination of NO donor DEAN, with the above-said inhibitors showed significant increase in tip cell sprouting ($n = 3$; $^{*}p<0.05$ vs control, $^{\#}p<0.001$ vs control). (Color figure online)

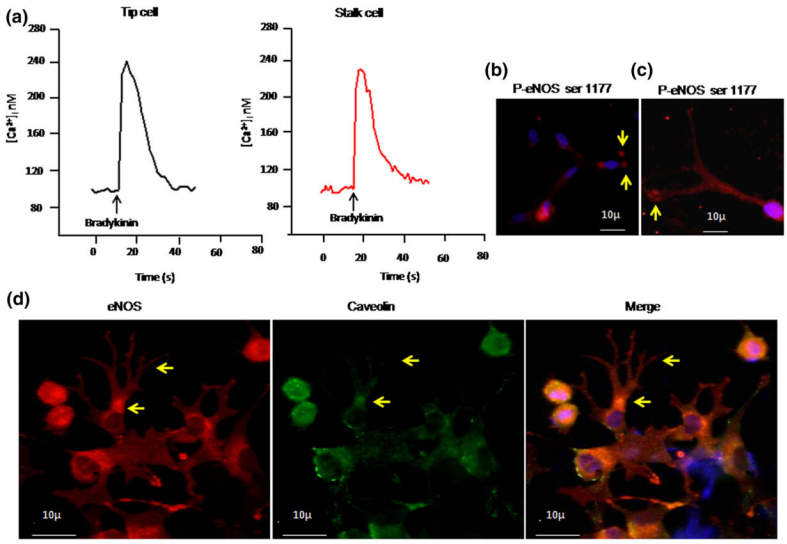

Fig. 9.

Calcium imaging in tip cells: **a** After 24 h of tip cell formation, EA.hy926 cells were incubated with 10 µM fura 2-AM dye for 30 min, followed by 30 min of washing in fura-free buffer. Images were acquired with the help of ANDOR CCD camera Luca-r attached with Olympus IX71, controlled through Andor IQ software (ANDOR technologies, USA). Bradykinin-induced calcium rise was measured by applying 1 µM of bradykinin. **b**–**d** Immunofluorescence imaging of P-eNOS and caveolin. BAECs were allowed to form tip cells. The cells were fixed, permeabilized, and incubated with P-eNOS ser 1177 primary antibody. **b** Active P-eNOS spots were observed in tip cells compared with that in stalk cells. **c** P-eNOS expression was found to be dominant at the apex of the tip cell (*yellow arrow*). **d** Immunofluorescence for both eNOS (*red*) and caveolin (*green*) was done, and the images were captured. Nuclear stain was done using DAPI (*blue*). The merged image demonstrates colocalization of eNOS and caveolin. (Color figure online)